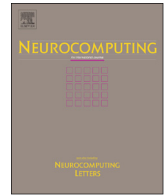




ELSEVIER

Contents lists available at ScienceDirect

Neurocomputing

journal homepage: www.elsevier.com/locate/neucom

A new ISR method based on the combination of modified K-SVD model and RAMP algorithm[☆]



Li Shang^{a,1}, Xin Wang^b, Yan Zhou^a, Zhanli Sun^c

^a Department of Communication Technology, Electronic Information Engineering College, Suzhou Vocational University, Suzhou 215104, Jiangsu, China

^b Simon Fraser University, 8888 University Drive Burnaby, B.C., Canada V5A 1S6

^c College of Electrical Engineering and Automation, Anhui University, Hefei 230039, Anhui, China

ARTICLE INFO

Article history:

Received 23 July 2014

Received in revised form

12 September 2014

Accepted 6 October 2014

Available online 2 December 2015

Keywords:

Image super-resolution reconstruction

Sparse representation

High resolution (HR)

Low resolution (LR)

K-Singular Value Decomposition (K-SVD)

Regularized adaptive matching pursuit

(RAMP)

ABSTRACT

A new Image Super-resolution Reconstruction (ISR) method combined a modified K-means based Singular Value Decomposition (M_K-SVD) model and Regularized Adaptive Matching Pursuit (RAMP) algorithm is proposed in this paper. In the M_K-SVD model, the maximum sparsity of sparse coefficients is considered. In the condition of the unknown sparsity of the original signals, RAMP algorithm can choose automatically and adaptively the candidate set, and utilize the regularization process to implement the final support set so as to finish accurately the task of signal reconstruction. Combined the advantages of M_K-SVD and RAMP algorithm, for LR images and High Resolution (HR) images, the LR and HR dictionaries are trained. And then, utilized the optimized LR sparse coefficient vectors and the HR dictionary, the HR image patches can be estimated. And considered the original locations of HR image patches to be restored, the LR images can be reconstructed. However, LR images contain much unknown noise, so, before training dictionaries, the LR images are first preprocessed by M_K-SVD model. In test, human-made LR images (i.e. natural images' degraded versions) and real LR images (i.e. millimeter wave images, MMW) are respectively used to testify our method proposed. Further, compared our ISR method with those of the basic K-SVD, Regularized Orthogonal Matching Pursuit (ROMP), RAMP, and Sparsity Adaptive Matching Pursuit (SAMP) and so on, experimental results testified the ISR validity of our method proposed. Meanwhile, the Signal Noise Ratio (SNR) criterion is used to measure restored human-made LR images, and the Relative Signal Noise Ratio (RSNR) criterion is used to test the quality of MMW image restored. Experimental results prove that our method is indeed efficient in the research field of ISR reconstruction.

© 2015 Published by Elsevier B.V.

1. Introduction

The spatial resolution of an image is an important measurement criterion of the image's equality. In generally, an image's spatial resolution means the minimized size can be distinguished clearly, which can be measured commonly using the spatial pixel density (i.e. pixels per inch, ppi) [1–3]. The higher the image resolution is, the larger the spatial pixel density is, and the smaller the reflective detail size in an image is, as well as the richer the image's detail is. Therefore, high resolution (HR) images are very useful in image processing field today [6–8]. However, in the practical process of imaging, the imaging result is degraded by

some factors, such as the imaging pattern, the nature weather condition, and the hardware devices et al, so, the observed image is in fact a Low Resolution (LR) one. To obtain the HR images from LR ones, the research of Image Super-resolution Reconstruction (denoted by ISR) has been an important subfield in image processing field at present [6–10]. The goal of ISR is to reconstruct the High Resolution (HR) image from a single or a series of low resolution images [11–17]. Currently, this ISR technology also has been used widely in image reconstruction and image compression, high definition digital TV, remote-sensing and radar images, medical diagnostics and so on [5–8]. To this day, many ISR methods have been proposed [1–8], and they are summarized mainly as frequency domain method and spatial domain method. But, the former's denoising capability is limited in application. Moreover, this method can not fuse the prior information of images, and it can not be constrained by regularized rules. Therefore, the latter's research work is mainly done now.

The published typical spatial domain based ISR methods are divided into mainly three classes, i.e., the interpolation based

[☆]Preliminary version of this manuscript has been selected as one of the best papers in International Conference on Intelligent Computing (ICIC 2014), 2014 (Paper ID: 127) and sub-selected in the Neurocomputing journal.

E-mail addresses: shangli0930@126.com (L. Shang), xwa49@sfu.ca (X. Wang), zhyang@jssvc.edu.cn (Y. Zhou), zhlsun2006@yahoo.com.cn (Z. Sun).

¹ Tel.: +86 512 6601584.

method, the reconstruction based method and the learning based method [2–8]. The first class methods are very simple. However, this class of methods can not introduce extra high frequency information, and the supposed prior model is usually unstable, so the interpolation efficiency is commonly bad [3]. The second methods first assume that LR images are obtained by making HR images geometry deformed, fuzzed and down-sampled, further, they utilize the fusion of multiple LR images to invert HR images. However, in this class of methods, the motion estimation and matching among frame images are very critical. But, the precise image matching relation is very difficult to obtain, moreover, with the increasing of the resolution multiple (commonly exceed 4 times), the matching relation with minor error will cause great degradation of images restored [18,19], thus, the matching relation is invalid. The last methods are learning based ones [15–18], which can obtain much more high-frequency information by training samples to learn the relation between LR image patches and HR image patches. At present, learning based ISR methods are thought as the hot research topics. Currently, typical learning based image ISR methods generally are summarized as samples based ones [19,20], Local Linear Embedding based Manifold Learning (LLE-ML) methods [19], Neighbor Embedding (NE) methods [21,22], K-Nearest Neighbor (K-NN) methods [21], Kernel ridge regression methods [23], wavelet coefficient dictionary methods [22], and sparse representation based methods [24,25] and so on. Among these typical ones, sparse representation based methods are the most popular and many ones also has been developed in restoring LR image s [24–29]. Sparse representation based theories can well solve many inverse problems existing in the fields of images. At present, among published sparse representation based algorithms, the K-means based Singular Value Decomposition (K-SVD) is such a typical one [30–35], and it has been used successfully in restoring, denoising and inpainting images. This method algorithm is an iterative method that alternates between sparse coding of the examples based on the current dictionary, and a process of updating the dictionary atoms to better fit the data [30]. The update of the dictionary column is combined with an update of the sparse representations, and thereby accelerating convergence can be done [36]. This K-SVD algorithm is very flexible and can work with any pursuit method (e.g. basis pursuit or matching pursuit).

Currently, in the common K-SVD algorithm, the over-complete dictionary is trained by using Orthogonal Matching Pursuit (OMP), Regularized OMP (ROMP) [14–16], Stage-wise OMP (StOMP) [15–16], Subspace Pursuit (SP), Compressive Sampling Matching Pursuit (CoSaMP) [6], Sparsity Adaptive Matching Pursuit (SAMP) [6,17,18], Regularized Adaptive Matching Pursuit (RAMP), et al., these algorithms are summarized as greedy matching pursuit ones [18,42–45]. However, algorithms of OMP, ROMP, StOMP and SP require in advance the sparsity of the original data to be known [18], at the same time, they also lack provable reconstruction quality [16,37–42]. The SAMP is effective in the case that the sparsity is unknown [6]. However, the SAMP method could not remove inappropriate atoms out once they were chosen [18]. The RAMP algorithm was proposed by Liu et al. [5] by combining the advantages of ROMP and SAMP. This method can approach the sparsity adaptively by accumulating a fixed unit of step size and adding the method of regularization to select the atoms again [5,17–18], and the selection of atoms in this method becomes more flexible.

In this paper, considering the advances of RAMP and K-SVD as well as the maximum sparsity of image feature coefficients, a modified K-SVD (M_K-SVD) denoising model is proposed and further used to implement the ISR task. This M_K-SVD model behaves better self-adaptively denoising property and almost independent of sparse priors. Here, LR images are first pre-processed by M_K-SVD model based on RAMP optimization

process. Further, utilized the idea of ISR technique and LR and HR dictionaries, trained by M_K-SVD model based on RAMP, the ISR task can be implemented well [35–52]. At the same time, in order to reduce the iteration time, LR dictionary and HR dictionary are also classed by using K-mean method. Then, using LR coefficients and HR dictionary learned, the HR image patches can be restored efficiently. In test, a simulation LR image and a real LR image called Millimeter Wave (MMW) image are respectively used to testify our image ISR method. Further, the validity of our method is also proved that it has better reconstruction efficiency than most of the available greedy algorithms, such as the basic K-SVD, ROMP, RAMP, and SAMP.

The remainder of this paper is organized as follows. Section 2 will restate relative greedy algorithms, such as ROMP, SAMP, RAMP and so on. Section 3 gives the description of basic K-SVD algorithm and the M_K-SVD denoising model respectively. Finally, some simulation experiments are discussed in Section 4 and some conclusions are obtained in Section 5.

2. Relative greedy algorithms

At present, the popular class of sparse recovery algorithms is based on the idea of iterative greedy pursuit, such as OMP, ROMP, StOMP, CoSaMP above mentioned. It is noted that the RAMP algorithm is the combined one of ROMP and SAMP algorithms, therefore, the ROMP, SAMP and RAMP algorithm are mainly discussed.

2.1. ROMP algorithm

ROMP is an iterative algorithm proposed by Needell et al. in 2009 [34–36], which is a variant of OMP. Defined a measurement matrix $\Phi \in R^{m \times n}$ with the Restricted Isometry Constant (RIC) δ_{2T} ($\delta_{2T} \in (0, C_T/(2C_T+1))$), the measure vector $x \in R^m$, and the support T of signal v , the ROMP algorithm is generalized as follows [17,18,34–36]:

Step 1. *Initializ*: Let the initial residual vector $r_t = y$, the index set $I_t = \emptyset$, and start the iteration counter with $t = 1$.

Step 2. *Identify*: Choose a set J of $|T|$ biggest absolute values of the observed vector $u = \Phi * r_t$.

Step 3. *Regularize*: Divide the set J into subsets J_k which satisfies the formula of $|u(i)| \leq 2|u(j)|$ for all $i, j \in J_k$, and choose the subset J_0 with the maximum energy of $\|u_{|J_0}\|$.

Step 4. *Update*: Set $I_t = I_{t-1} \cup J_0$. Calculate the new approximation by solving the least square equation

$$v_t = \underset{c}{\operatorname{argmin}} \|y - \Phi_{I_t} c\|_2 \quad (1)$$

and update the residual: $r_t = x - \Phi_{I_t} v_t$.

Step 5. *Ending*: Check the stopping criterion, if not, then keep increasing $t = t + 1$. When ROMP algorithm halts, the residual vector r_t is calculated by the form of $\|r_t\|_2 < K_{1,T} \times \eta$, where η is a minor positive threshold, and $K_{1,T}$ is defined by the following formula:

$$\begin{cases} K_{1,T} = \frac{C_T(1-\delta_{2T})}{C_T(1-\delta_{2T})-\delta_{2T}} \\ C_T = \frac{1}{5.6\sqrt{\log |T|}} \end{cases} \quad (2)$$

Then, the estimated \hat{v} of the ROMP algorithm will obey the rule of $\|v - \hat{v}\|_2 K_{2,T} \times \eta$, where $K_{2,T} = \sqrt{2}(K_{1,T} + 1)$.

It is well known that the main difference between OMP and ROMP is the identification and regularization steps. In stead of choosing only one biggest correlation between the residual and columns of the matrix at each iteration as in OMP, ROMP choose a set of $|J_0|$ coefficients from $|J|$ biggest absolute coefficients of

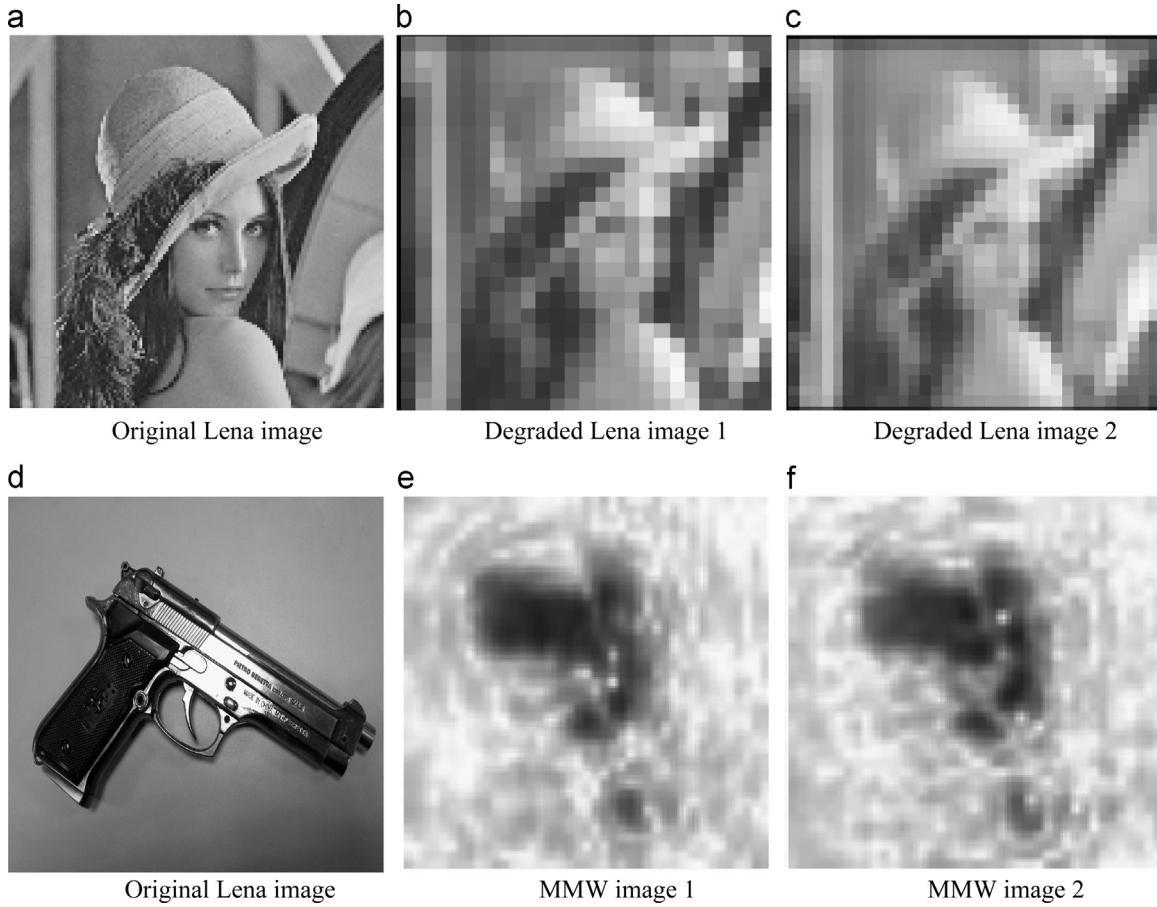


Fig. 1. The original images and the corresponding degraded images. (a) The original Lena image; (b) and (c) artificial LR images, i.e., noise versions of Lena image with different noise level. (d) The imaging target of MMW image; (e) and (f) Real LR images, i.e., MMW images.

$\Phi * r_t$. By this way, ROMP can recover signals perfectly without going through all $|T|$ iterations. As a result, ROMP performs much faster than OMP [36].

2.2. SAMP algorithm

ROMP can yield exact sparse recovery in the noiseless case, but it needs in advance to know the prior sparsity level K , so it is limited in practice. To avoid this defect, SAMP was proposed by Do Thong et al. [15]. Let x denote the measure vector, y denote the sampled vector, Φ be the sampling matrix, and s be the size of the finalist in the first stage of SAMP, referring to the document [17], the SAMP algorithm is described briefly as follows:

Step 1. Let the initial residue vector $r_0 = y$, the support set $F_0 = \Phi$, the iteration index $t = 1$, the stage index $j = 1$, and the initial step size $\Gamma = s$.

Step 2. Find the candidate set S_k by choosing the Γ largest atoms in the absolute values of $\langle r_{k-1}, \Phi \rangle$, i.e., $S_k = \text{Max}(|\Phi * r_{k-1}|, \hat{L})$ is the preliminary test.

Step 3. Get the candidate set C_k by $C_k = F_{k-1} \cup S_k$.

Step 4. Compute $\hat{x}_{C_k} = \Phi_{C_k}^\dagger \cdot y$ and select the support set F_k by choosing the Γ largest atoms with the value of \hat{x}_{C_k} .

Step 5. Compute residue r by the formula of $r = y - \Phi_F \Phi_F^\dagger y$ where Φ_F is the sampling matrix corresponding to the final test set F . Here F is calculated by $F = \text{Max}(|\Phi_{C_k}^\dagger y|, \hat{L})$, where $\Phi_{C_k}^\dagger$ is the sampling matrix corresponding to the candidate index C_k .

Step 6. If $\|r\|_2 \geq \|r_{k-1}\|_2$, going to the stage switching. And updating the stage index $j = j + 1$, and the size of finalist $\hat{L} = j \times s$.

Else, updating the finalist $F_k = F$ and the residue $r_k = r$, and then beginning the next loop $t = t + 1$. And go to Step 1 to continue a new stage iteration process. Output the prediction of non-zero coefficients, which is calculated by $\hat{x} = \Phi_F^\dagger y$.

Step 7. If the halting condition $\|r\|_2 < \varepsilon$ is true (ε is the threshold), then the iteration is end, else if beginning the steps from the Step 6. And it is noted that $\varepsilon = 0$ for noiseless measurements and ε can be chosen as the noise energy for noisy measurements.

The SAMP algorithm can reconstruct the signal by accumulating a fixed unit to step size to approach the sparsity adaptively when the sparsity is unknown. Another is that atoms are chosen accurately by backtracking method. However, SAMP algorithm has also some defects [48–52]. For example, since the increase unit of step size is fixed, the length of step size Γ might become larger than the magnitude of sparsity if the increase unit s is too large. Besides, there are repeated computations for atom selections during the adjacent iteration stages [17,18,53–55]. It is inevitable because there is the backtracking idea of subspace pursuit.

2.3. RAMP algorithm

RAMP algorithm is a new greedy algorithm, which combines the advantages of ROMP and SAMP, and ensures both the whole optimization and the convergent speed [3,5,16]. Let ε_1 and ε_2 denote respectively the iteration times and the threshold of stage switch. x and y are still the measurement vector and the observation vector respectively. Then, referring to ROMP and SAMP algorithm, RAMP algorithm used in this paper is generalized in main as follows:

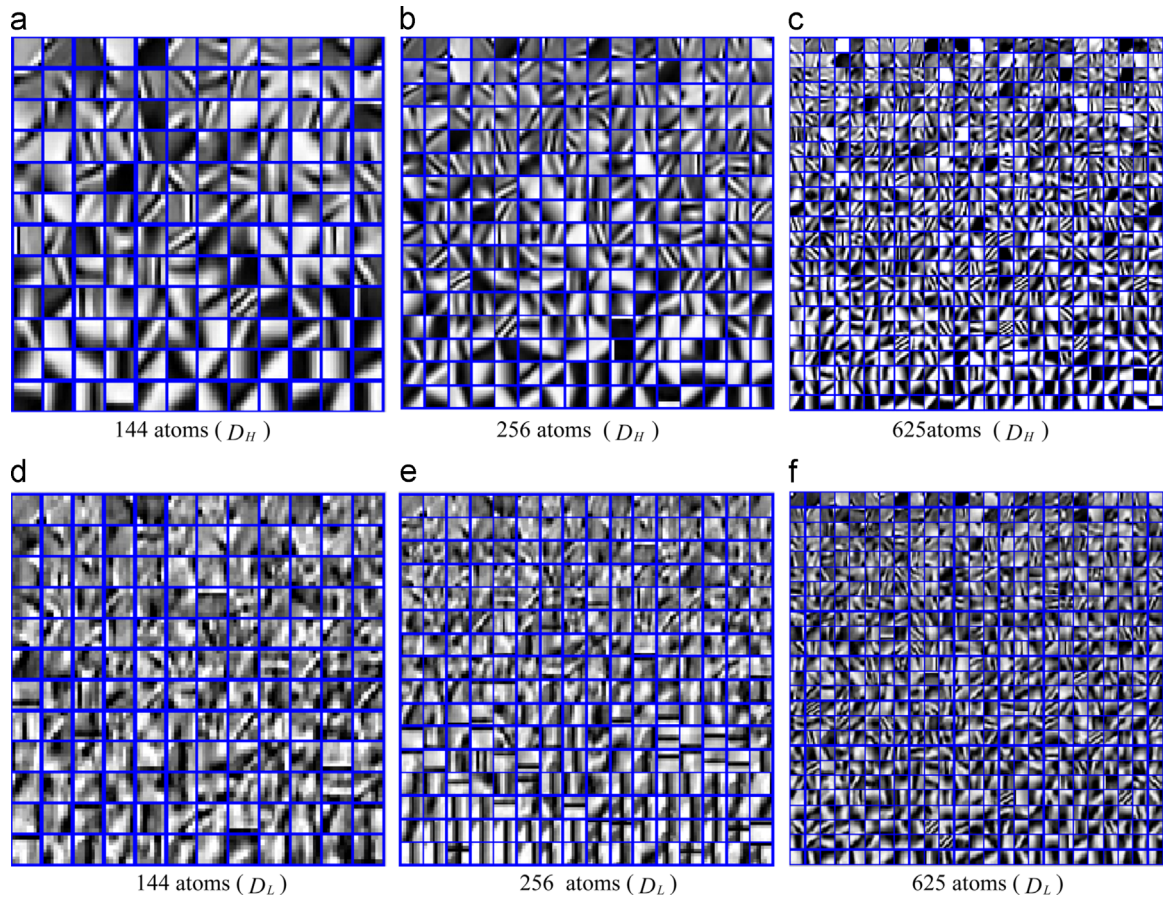


Fig. 2. Lena image's HR and LR dictionaries with different numbers of atoms of M_K-SVD model. The first row: HR dictionaries; The second row: LR dictionaries. (a) 144 atoms (D_H) (b) 256 atoms (D_H) (c) 625atoms (D_H) (d) 144 atoms (D_L) (e) 256 atoms (D_L) (f) 625 atoms (D_L).

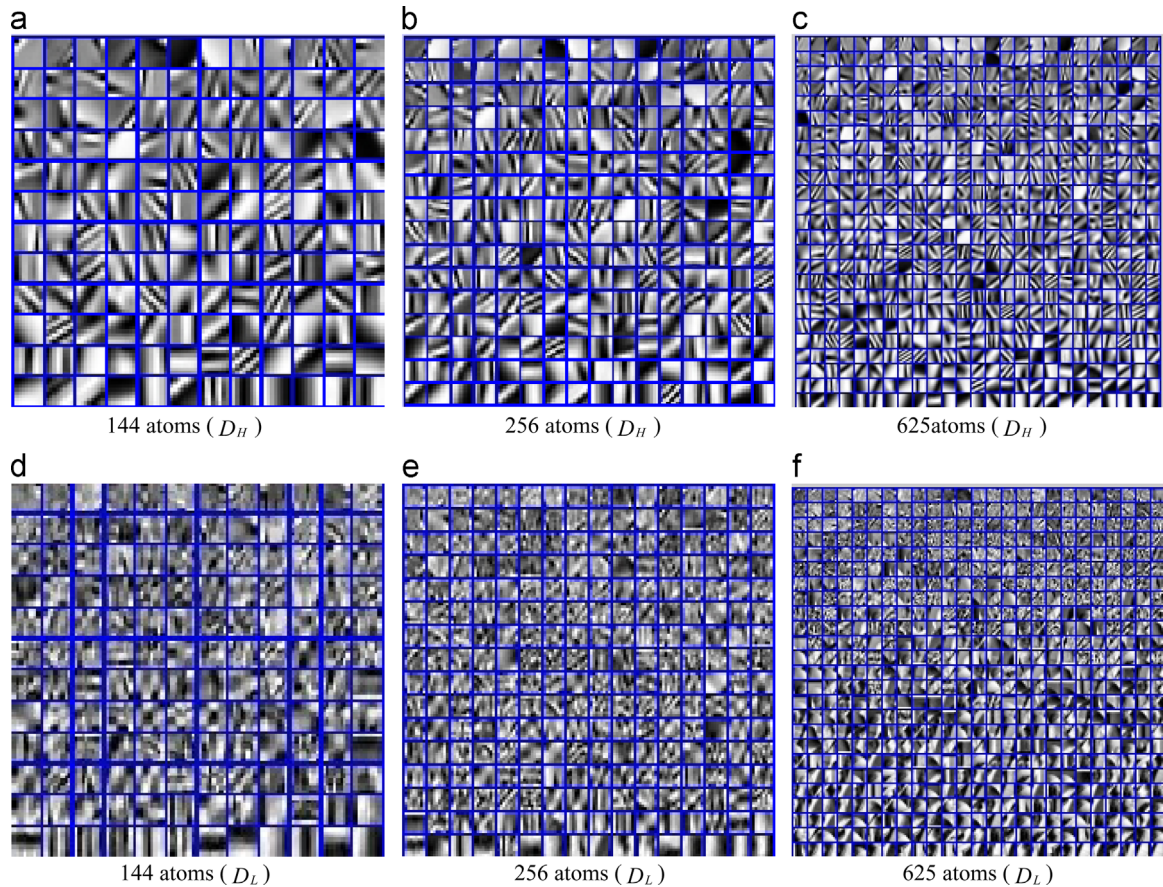


Fig. 3. Lena image's HR and LR dictionaries with different dimension of atoms of basic K-SVD model. The first row: HR dictionaries; the second row: LR dictionaries. (a) 144 atoms (D_H) (b) 256 atoms (D_H) (c) 625atoms (D_H) (d) 144 atoms (D_L) (e) 256 atoms (D_L) (f) 625 atoms (D_L).

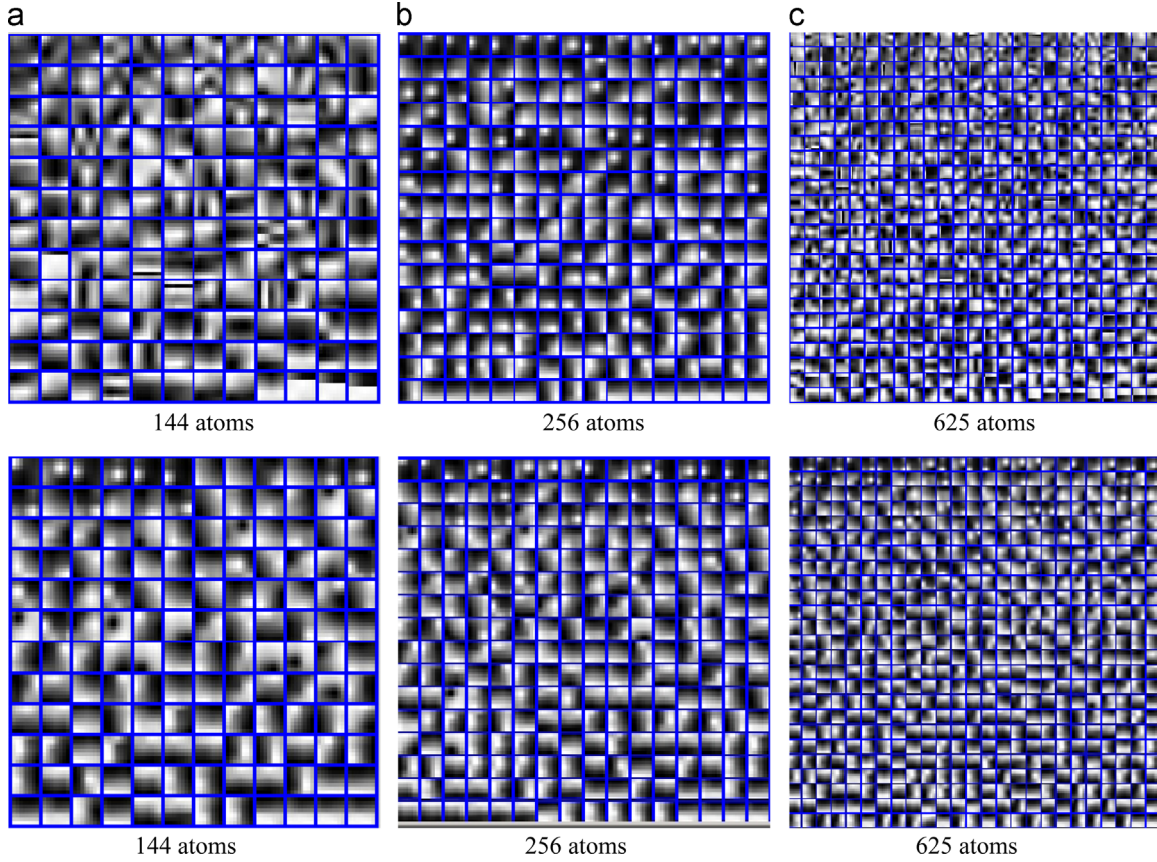


Fig. 4. MMW Dictionaries with different numbers of atoms obtained by different K-SVD models. The first row: dictionaries of the M_K-SVD model. The second row: dictionaries of the basic K-SVD model. (a) 144 atoms (b) 256 atom (c) 625 atoms.

Step 1. Initialized setting. Let the initial residue $r_0 = y$, the step size $\eta \neq 0$, the stage index $j = 1$, the iteration time $t = 1$, and the index set $J \neq \emptyset$, $\Lambda = \emptyset$.

Step 2. If the residue $\|r\|_2 \leq \varepsilon_1$, stopping the iteration. The reconstruction can be implemented by atoms trained. Else, go to Step 3.

Step 3. Using Eq. (3) to calculate relative coefficient set u , and the L biggest indexes in u are saved in J .

$$u = \{u_j | u_j = |\langle r, \Phi_j \rangle|, j = 1, 2, \dots, N\} \quad (3)$$

Step 4. Regularized relative coefficients of atoms responding to the index set J , and saved the regularized results in set J_0 . In set J_0 , all coefficients satisfy $|u(i)| \leq 2|u(j)|$ ($i, j \in J_0$), and choose J_0 with the maximal energy $\|u|_{J_0}\|_2$.

Step 5. Updating the support set φ_Λ , where $\Lambda = \Lambda \cup J_0$;

Step 6. Using Eq. (4) to obtain \hat{x} , and updating the residual using Eq. (5):

$$u = \hat{x} = \operatorname{argmin}_{i \in R^\Lambda} \|y - \varphi_\Lambda x\|_2 \quad (4)$$

$$r_{new} = y - \varphi_\Lambda \hat{x} \quad (5)$$

Step 7. If $\|r_{new} - r\|_2 \leq \varepsilon_2$, let $j = j + 1$, $\eta = \eta * j$. Then go to Step 3. Else, let $r = r_{new}$, $t = t + 1$, go to Step 2.

According to the above steps, it is clear that by the setting threshold ε_1 and ε_2 , RAMP algorithm can define self-adaptively whether to adjust the current step size so as to define whether the next stage or next iteration is implemented or not [5–9].

3. The modified K-SVD denoising model

3.1. K-SVD algorithm description

K-SVD algorithm is flexible and works in conjunction with any pursuit algorithm [32–34], and it is designed to be a truly direct generalization of the K-Means [33–38]. Currently, it is also taken for a typical sparse representation method based on dictionary learning. In this case, the small amount of signal values can be reconstructed accurately when the signal is sparse. Set D to be the dictionary matrix with K prototype signal atoms for columns, Y to be the sparse linear combination of these atoms, and S is the coefficients of sparse representations, the object function of K-SVD is defined as

$$\min_{D, S} \{\|Y - DS\|_F^2\} \quad (6)$$

subject to $\forall_i, \|s_i\|_0 \leq T_0$. In minimize the expression in Eq. (6) iteratively, D is fixed to find the best coefficient matrix S that can be found. Considered column representation, this cost function can be rewritten as

$$\|Y - DS\|_F^2 = \sum_{i=1}^N \|y_i - Ds_i\|_2^2 \quad (7)$$

subject to $\forall_i, \|s_i\|_0 \leq T_0$. This problem is adequately addressed by the pursuit algorithms [33]. In Eq. (7), let d_k denote the k th column of D , s_k^i be the i th row of sparse coefficients corresponding to d_k (i.e. s_i is the i th column in S). Then Eq. (7) is rewritten as

$$\|X - DS\|_2^2 = \|Y - \sum_{j=1}^K d_j s_j^i\|_2^2 = \left\| X - \sum_{j \neq k} d_j s_j^i \right\|_2^2$$



Fig. 5. Reconstructed results of Lena LR images with different noise level by different algorithms. (a) 0.01 noise variance (b) 0.8 noise variance (c) 1.5 noise variance (d) 0.01 noise variance (e) 0.8 noise variance (f) 1.5 noise variance (h) 0.01 noise variance (i) 0.8 noise variance (j) 1.5 noise variance (k) 0.01 noise variance (l) 0.8 noise variance (m) 1.5 noise variance.

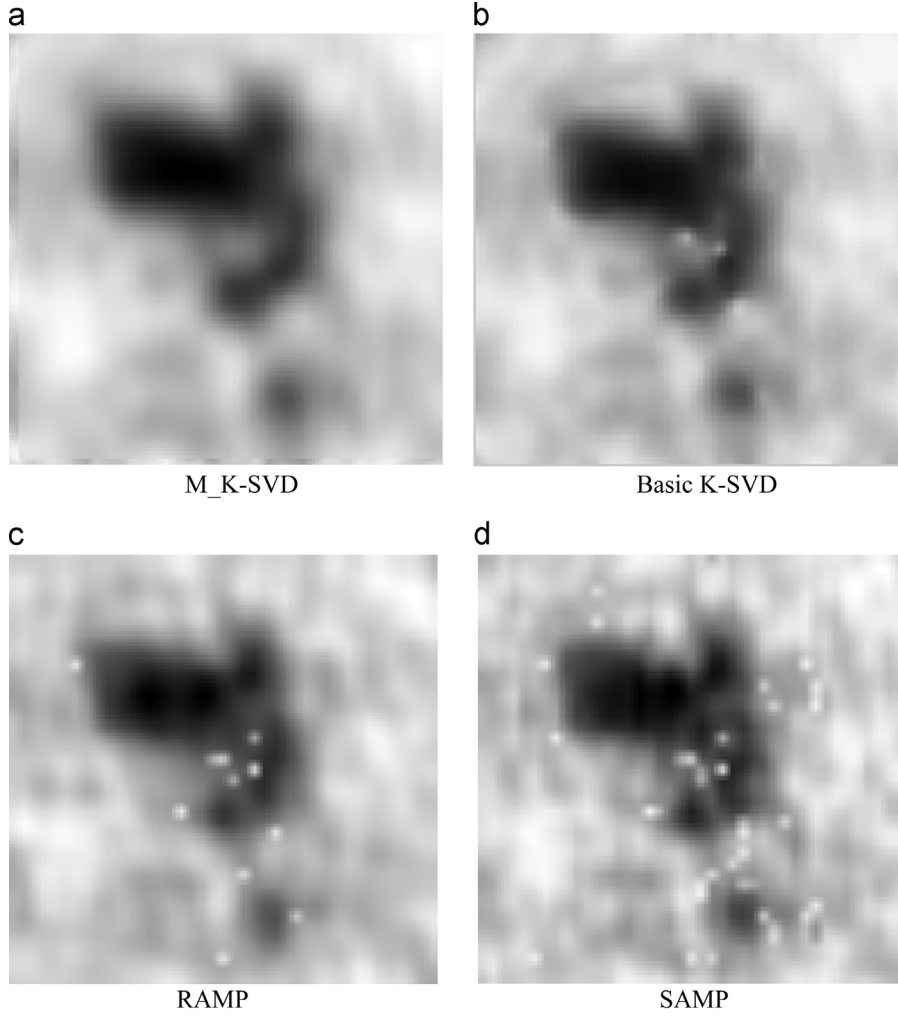


Fig. 6. Dictionary with 256 atoms and denoised results of MMW image 1 by using different algorithms. The first row: reconstructed of MMW image 1 (see Fig. 1(e)). The second row: reconstructed of MMW image 2 (see Fig. 1(f)).

$$-d_k s_T^k \|\hat{E}\|_F^2 = \|E_k - d_k s_T^k\|_F^2 \quad (8)$$

where the matrix E_k stands for the error for all the N examples when the k th atom is removed [33]. For Eq. (7), it is not directly used SVD algorithm to update d_k . To solve this problem, ω_i is defined as the group of indices pointing to examples $\{y_i\}$ that use the atom d_k , thus, $\omega_k = \{i | 1 \leq i \leq K, s_T^k(i) \neq 0\}$. Define Ω_k as a matrix with the size of $N \times |\omega_k|$, with ones on the $(\omega_k(i), i)$ -th entries, and zeros elsewhere. Let $s_R^k = s_T^k \Omega_k$ and $Y_k^R = Y \Omega_k$ with the size of $n \times |\omega_k|$, thus, the error $E_k^R = E_k \Omega_k$ can be obtained. So, Eq. (8) is rewritten as

$$\|E_k \Omega_k - d_k s_T^k \Omega_k\|_2^2 = \|E_k^R - d_k s_R^k\|_2^2 \quad (9)$$

For Eq. (9), it can be done directly via SVD algorithm. Taking the restricted matrix E_k^R , SVD decomposes it to $E_k^R = U \Delta V^T$. Here, the vector d_k is defined as the first column of matrix U , and s_R^k is defined as the first column of V multiplied by $\Delta(1, 1)$. While K-Means applies K computations of means to update the codebook, the K-SVD obtains the updated dictionary by K-SVD computations, each determining one column.

3.2. M_K-SVD denoising model

Especially, for images with large noise variance or low-resolution, K-SVD has better denoising robustness. Assumed that x_i an image patch (column vector), and consider a noisy version of it,

$y_i = x_i + \sigma$, contaminated by an additive zero-mean white Gaussian noise with standard deviation σ . The maximum a posteriori (MAP) estimator for denoising this image patch is built by solving the following form

$$\hat{s} = \arg \min_s \|s\|_0 \quad (10)$$

subject to $\hat{s}_i = \|Ds_i - y_i\|_2^2 \leq T_r$, where $T_r > 0$ is a small threshold, dictated by σ and the number of atoms K . Thus, the denoised image patch is thus given by $x_i = D\hat{s}_i$. In practice, the optimization task of \hat{s}_i denoising model is changed to be

$$\hat{s}_i = \arg \min_s \|y_i - Ds_i\|_2^2 + \mu \|s_i\|_0 \quad (11)$$

where Eq. (11) is the denoising model described in document [15], namely the basic KSVD denoising model used in this paper. Here, to solve Eq. (11), the OMP algorithm is used because of its simplicity. However, the maximum sparsity can not be ensured in Eq. (10). To solve this question, a M_K-SVD denoising model is proposed by us, which is described as in the following formula [31]:

$$J(\hat{D}, \hat{S}) = \arg \min_{\hat{S}, \hat{D}} \left[\lambda \|Y - X\|_2^2 + \sum_{ij} \mu_{ij} \|S_{ij}\|_0 + \gamma \sum_{ij} (D_{ij}^T D_{ij}) + \sum_{ij} \|DS_{ij} - R_{ij} X\|_2^2 \right] \quad (12)$$

Table 1
SNR values of restored images obtained by different algorithms (LR images of Lena).

Standard deviations	Algorithms					
	M_K-SVD	Basic K-SVD	RAMP	SAMP	ROMP	LR images (Lena)
0.05	11.898	5.136	9.626	5.728	6.817	0.516
0.1	11.898	5.132	9.622	5.725	6.813	0.515
0.5	9.532	4.532	7.072	4.275	5.382	0.862
1.0	7.271	3.281	5.857	2.621	3.627	0.980
1.5	6.826	3.012	4.718	1.136	2.428	0.507
2.0	3.468	1.192	1.503	0.837	1.263	< 0
3.0	1.065	0.826	0.878	0.062	< 0	< 0
4.0	0.827	0.803	< 0	< 0	< 0	< 0
5.0	0.827	0.803	< 0	< 0	< 0	< 0

In Eq. (12), a larger unknown image patch set X , namely the reconstructed image patches, and the measured image set Y , namely the LR image patches, are also considered. The first term is the log-likelihood global force that demands the proximity between the measured image Y and its denoised version X . The second and the third terms are parts of the image priors that makes sure that, in the constructed image patch set X , each patch X_{ij} with the size $p \times p$ pixels in every location has a sparse representation with bounded error, where X_{ij} is calculated by using the Equation of $X_{ij} = R_{ij}X$. Matrix R is a $p \times N$ matrix that extracts the (i, j) block from an image with the size $N \times N$ pixels. For an $N \times N$ image set X , the summation over i, j includes $(N - p + 1)^2$ items, considering all image patches with the size of $p \times p$ pixels in X overlaps. The coefficients μ_{ij} must be location dependent so as to comply with a set of constraints of the formula of $\|DS_{ij} - X_{ij}\|_2^2 \leq T_r$.

3.3. Denoising LR image by M_K-SVD model

In training the dictionary, each LR image is sampled randomly image patches of size $p \times p$ 5000 times, and each image patch is converted into a column, thus, the image patch set $Y = \{y_i\}_{i=1}^M$ is obtained, where y_i is the i th overlap image patch, and M is the number of overlap image patches, which can be calculated by $(N - p + 1)^2$. For the set Y , again sampling randomly M' ($M' < M$) times to obtain training set $Y' = \{y'_i\}_{i=1}^{M'}$, where y'_i is the i th training sample. Thus, the training sample set Y' can be obtained, and using the following steps, Eq. (11) can be minimized.

Step 1. Fixed dictionary D and training sparse coefficient matrix \hat{S} . As to the objective function $\forall i, \hat{S}_i = \arg \min_{S_i} \|DS_i - Y_i\|_2^2 + \mu_i \|S_i\|_0 + \gamma \sum_{ij} (D_{ij}^T D_{ij})$, and using RAMP algorithm to implement sparse coding and obtain sparse coefficients $\hat{S} = \{\hat{S}_i\}$.

Step 2. Let $S = \hat{S}$, and update dictionary. Define $\omega_k = \{i | 1 \leq i \leq K, (S_i)_R^k \neq 0\}$ as the group of indices pointing to examples $\{Y_i\}$ that use the atom vector d_k , i.e., those $(S_i)_R^k$ is nonzero. Compute the error matrix \hat{E}_k by the form of $\hat{E}_k = Y - \sum_{i \in \omega_k} d_i (S_i)_R^k$. Restrict \hat{E}_k by choosing only the columns corresponding to ω_k and \hat{E}_R^k obtained, and then apply SVD to decompose $\hat{E}_R^k = U \Delta V^T$. Finally, update vector $(S_i)_R^k$ as the first column of V multiplied by $\Delta(1, 1)$. If \hat{E}_k satisfy the error condition, then the training loop stops.

Step 3. For dictionary \hat{D} obtained in Step 2, utilize RAMP algorithm described in Subsection 2.3 to learn all overlap image patch set Y , and obtain estimated sparse coefficient matrix \hat{S} .

Step 4. Fixed dictionary matrix \hat{D} and sparse coefficient matrix \hat{S} , and then update matrix X by the formula of $\hat{X} = \arg \min_{X_j} \lambda \|Y - X\|_2^2 + \sum_{ij} \|\hat{D} \hat{S}_{ij} - R_{ij} X\|_2^2$.

Table 2
RSNR values of different algorithms of restored MMW images.

Algorithms	MMW image 1 Restored results	MMW image	MMW image 2 Restored results	MMW image
M_K-SVD	17.36	12.37	17.42	12.52
Basic K-SVD	13.23		13.36	
RAMP	15.68		15.84	
SAMP	14.52		14.67	
ROMP	14.61		14.73	

Step 5. Compute the estimation \hat{Y} of Y by $\hat{Y} = \hat{D} \hat{S}$. Then the denoised image \hat{X} can be obtained by $\hat{X} = \left(\lambda I + \sum_{ij} R_{ij}^T R_{ij} \right)^{-1}$

$\left(\lambda \hat{D} \hat{S} + \sum_{ij} R_{ij}^T \hat{D} \hat{S}_{ij} \right)$, where I is unit matrix.

Using above described steps of K-SVD denoising model, a degraded image can be effectively and self-adaptively denoised. Based on this idea, utilizing the self-adaptively denoising advantage of K-SVD model, LR images are preprocessed by it before training LR dictionary.

4. Experimental results and analysis

4.1. Learning HR and LR dictionaries

In test, several degenerated versions of Lena image and real MMW images were used. The original Lena image with 128×128 pixels and imaging object of MMW imaging system were shown in Fig. 1(a) and (d). First, for Lena image, the motion blur operator was used, namely, PSF function was simulated. Next, for the blurred results of PSF, the down sampling method and Gaussian mask method were utilized. Further, to get degraded greatly images, the Gaussian blur method was used, thus, artificial LR images were obtained. Here, in implementing PSF function, the filter type was selected as Gaussian low-pass filter, and this filter size was chosen as 7×7 pixels. In down sampling processing, the linear type was chosen, and the extracting pixel scalar was set to be 5. Otherwise, different standard deviations of Gaussian kernel were considered in Gaussian blur processing.

By the degraded processing above-mentioned, some degenerated versions of Lena image could be obtained, for example, two degraded Lena images are shown in Fig. 1(b) and (c). The real LR images used in this paper were MMW images, which were generated by the MMW imaging system developed by our research group cooperated with MMW Lab. of Southeast University. However, the size of a MMW image obtained by our MMW imaging system was 41×41 pixels, and such MMW image in fact is very small in test, so, in application, in order to obtain better reconstruction results, the MMW image's size was usually expanded to 128×128 pixels or larger size. In test, two MMW images are used as shown in Fig. 1(e) and (f). From Fig. 1, clearly, LR images' equality is much worse than HR images, many image details are lost. Therefore, it is necessary to do the research task of super-resolution reconstruction of LR images.

In implementing the task of image reconstruction, four Lena LR images and MMW images were used as input images. The number of atoms is selected as 256. And first, the M_K-SVD denoising model was used to pre-process LR images in advance. And then, the denoised images were thought to be LR images in our test. To reduce computation time, the idea of sampling random image patches was considered. Here, each HR and LR image were both sampled 5000 times with 8×8 image patches with overlap of

three pixels between adjacent patches, thus the LR and HR image patch set with 64-dimension could be obtained and were denoted by X_L and X_H respectively. For Lena images, the D_H and D_L dictionary with different atom numbers obtained by the M_K-SVD algorithm based on RAMP optimization rule are shown in Fig. 2(a)–(c) and (d)–(f) in order. For comparison, in the same condition, those dictionaries obtained by the basic K-SVD model are learned and shown in Fig. 3 in order. For MMW images, the clear imaging object is unknown in fact, so, HR dictionaries can be obtained and only LR dictionaries with different dimensions of MMW images were discussed. The corresponding D_L dictionaries with 144, 256 and 625 atoms, obtained by the M_K-SVD model and the basic K-SVD model, are respectively shown in Fig. 4. Compared dictionaries of MMW images and those of Lena's LR images, it is clear to see that because of the much worse resolution of MMW images, the former behave more ambiguous orientation.

From Figs. 2 and 3, it is clear to see that, no matter what kind of K-SVD model, in different numbers of atoms, D_H dictionaries all have distinct orientation, locality and spatiality as those obtained in documents [39,41]. And regardless the number of atoms, compared D_L dictionaries of the M_K-SVD model and those of the basic model, it is also easy to see that the former behaves more certain orientation than the latter. For LR dictionaries of MMW images, the same comparison result can also be obtained in despite of unknown noise contained in LR dictionaries. Otherwise, in test, it also noted that the training time of M_K-SVD model based on RAMP algorithm is also less than that of the basic K-SVD model based on OMP optimization.

Here, it should be noted that because of much unknown noise existed in original LR images, especially for real LR images, such as MMW images, the quality of LR images are greatly worse. To get better LR reconstruction effect, before training LR dictionaries, they were preprocessed in advance by the M_K-SVD denoising model. Then, the denoised LR images are confirmed to be LR image data used to learn LR dictionaries. And then, considered the idea of image ISR described in document [8], the image ISR task can be implemented by using the trained HR dictionary D_H and the optimal sparse coefficient vector \hat{S}^* of LR images learned by our method. And the detail of reconstruction will be discussed in Subsection 4.2.

4.2. Image reconstruction results

As described in published documents of ISR researches [29–33], utilized the learned HR dictionary and the optimized feature coefficient vector of LR images, the HR image patches can be reconstructed by the estimation form of $\hat{X} = D_H \hat{S}^*$. And then, considered each image patch's original position in the clear HR image, these image patches is again put into the HR image X_0 . At the same time, for the lapped pixels, the mean pixel value is used as the restored pixel value. In test, the ISR work of artificial LR images, namely Lena LR images, was first discussed so as to testify our method's effect. In the stages of degrading Lena images described in Subsection 4.1, in Gaussian blur processing, different standard deviations were considered, however, limited by the length of the paper, the ISR results of our method, corresponding to Lena LR images with 0.1 and 0.5 and 1.0 standard deviations, are shown in Fig. 5(a)–(c). Meanwhile, for comparison, in the same experimental condition, the ISR results of Lena LR images, obtained by algorithms of basic K-SVD, ROMP, RAMP, and SAMP are also given in Fig. 5 in order. And the ISR results of MMW images, obtained by the above-mentioned algorithms, are shown in Fig. 6.

From Fig. 5, clearly, no matter what kind of algorithms, it can be seen that the smaller the standard deviations of Gaussian kernel

(i.e. image deviations) is, and the better the visual effect of corresponding restored images of Lena is. When the noise level exceeds 2, the structure and contour of restored images obtained by our method are better than other methods discussed here. In a way, this also testifies that our method behaves certain robust to noise. But, when noise level is set to be 5, the restored effect of all ISR algorithms are all worse. However, these experiment results in some ways prove the validity and feasibility in image reconstruction of our method.

Meanwhile, according to Fig. 5, it is difficult to distinguish each algorithm's efficiency only in terms of the visual effect. Therefore, to further testify the super-resolution efficiency of our method proposed here, the equality of reconstructed LR images, obtained by different algorithms above-mentioned, were evaluated by the criterion of Signal Noise Ratio (SNR). However, it is noted that the original imaging object of the MMW image is unknown and there is much noise existed in the MMW image, so the quality of restored MMW image can not be measured by SNR criterion. Here, the Relative SNR (RSNR) criterion is used to estimate the MMW image. And the SNR and RSNR values are calculated by using the following formulas:

$$\begin{cases} \text{SNR} = 10 \log_{10} \frac{\sum_{i=1}^N \sum_{j=1}^M I_{ij}^2}{\sum_{i=1}^N \sum_{j=1}^M (I_{ij} - \bar{I}_{ij})^2} \\ \text{RSNR} = \frac{1}{\sqrt{NM}} \left[\sum_{i=1}^N \sum_{j=1}^M \hat{I}(i,j) \right] / \sqrt{\sum_{i=1}^N \sum_{j=1}^M [\hat{I}(i,j) - \bar{I}(i,j)]^2} \end{cases} \quad (13)$$

where $I(i,j)$ denotes the input image with the size of $N \times M$, $\hat{I}(i,j)$ denotes the reconstructed image and $\bar{I}(i,j)$ denotes the mean of $I(i,j)$. $\hat{I}(i,j)$ and $\bar{I}(i,j)$ behave the same size as $I(i,j)$.

Utilizing Eq. (13), the SNR values of restored images of Lena with different noise level are calculated and listed in Table 1, and the values of RSNR two MMW images are listed in Table 2. From Table 1, it is clear to see that, for each algorithm, the smaller the noise level is, and the larger the SNR is. At the same time, with the noise level increasing, no matter what kind of algorithms, the SNR values decrease. In the same noise level condition, it is also easy to see that SNR values of our method proposed are the largest, ones of RAMP algorithm are the second, and ones of the basic K-SVD are the smallest. Therefore, according to the visual effect shown in Fig. 5 and SNR values listed in Table 1, it can be concluded that our M_K-SVD method is efficient and feasible in processing the ISR task of LR images.

And From Table 2, for MMW images, in terms of RSNR values obtained by different algorithms, the same conclusions as artificial LR images can be obtained, which further proves that the M_K-SVD model can assuredly restore real LR images and is applicable in practice. Moreover, compared restored MMW images shown in Fig. 6 with original MMW images shown in Fig. 2, it can be seen that the noise in background has been reduced greatly and the contour of each MMW image restored is clearer and easier to recognition. So, based on test results, it can be concluded that in the image ISR task of LR images, our method proposed outperforms truly other algorithms discussed in this paper.

5. Conclusions

A novel image super-resolution reconstruction method combining a modified K-SVD (denoted by M_K-SVD) model and the RAMP algorithm is proposed in this paper. To improve the quality of reconstructed images, before training LR dictionaries, much unknown noise existed in LR images are first preprocessed by M_K-SVD model. Then, the HR and LR dictionary pairs are learned respectively by using M_K-SVD model based on the RAMP optimized process. After obtaining LR and HR dictionaries, utilizing

usual ISR idea, the ISR task can be implemented well by using HR dictionary and the sparse coefficients of LR images. In test, artificial LR images (i.e., degraded images of Lena with different noise variances) and real LR images (i.e. MMW images) are both used. The restored images of Lena and MMW are measured respectively by the SNR criterion and RSNR criterion. Experimental results shown that our ISR method proposed here can restore LR images efficiently Further, compared with ISR methods of the basic K-SVD, ROMP, RAMP and SAMP, experimental results also show that our method behaves in indeed the best effect in the image ISR task.

Acknowledgments

This work was supported by two National Natural Science Foundation of China (Grant nos. 61373098 and 61370109), the grant from Natural Science Foundation of Anhui Province (No. 1308085MF85), and the Innovative Achievement Foundation of Soochow Vocational University (No. 2011SZDCC06).

References

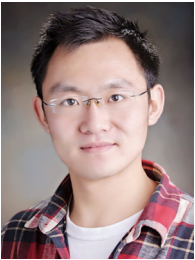
- [1] Q.S. Lian, J.Q. Zhang, S.Z. Chen, Single image super-resolution algorithm based on two-stage and multi-frequency-band dictionaries, *ACTA Autom. Sin.* 39 (8) (2013) 1310–1320.
- [2] G.L. Sun, Z.B. Shen, Image super-resolution reconstruction based on multi-groups of coupled dictionary and alternative learning, *J. Appl. Sci. Electron. Inf. Eng.* 30 (6) (2012) 642–648.
- [3] D. Needell, J.A. Tropp, CoSaMP: iterative signal recovery from incomplete and inaccurate samples, *Appl. Comput. Harmon. Anal.* 26 (3) (2008) 301–321.
- [4] E.J. Candes, T. Tao, Near-optimal signal recovery from random projections: Universal encoding strategies, *IEEE Trans. Info. Theory* 52 (2) (2006) 5406–5425.
- [5] Ya-xin Liu, Rui-zhen Zhao, Shao-hai Hu, Chun-hui Jiang, Regularized adaptive matching pursuit algorithm for signal reconstruction based on compressive sensing, *J. Electron. Inf. Technol.* 32 (11) (2010) 2713–2717.
- [6] N. Nguyen, D.T. Tran, Sparsity adaptive matching pursuit algorithm for practical compressed sensing, in *Proceedings of the 42nd Asilomar Conference on Signals, Systems and Computers*, Oct. 26–29, Pacific Grove, CA, pp. 581–587, 2008.
- [7] J. Tropp, A. Gilbert, Signal recovery from random measurements via orthogonal matching pursuit, *IEEE Trans. Inf. Theory* 53 (2) (2007) 4655–4666.
- [8] J. Sun, Z.B. Xu, H.Y. Shum, Gradient profile prior and its applications in image super-resolution and enhancement, *IEEE Trans. Image Process.* 20 (6) (2011) 1529–1542.
- [9] D.S. Huang, J.X. Min, A new constrained independent component analysis method, *IEEE Trans. Neural Netw.* 18 (5) (2007) 1532–1535.
- [10] Z.L. Sun, An extension of MISEP for post-nonlinear-linear mixture separation, *IEEE Trans. Circuits Syst. Part II: Express Briefs* 56 (8) (2009) 654–658.
- [11] D.S. Huang, W. Jiang, A general CPL-AdS methodology for fixing dynamic parameters in dual environments, *IEEE Trans. Syst. Man Cybern.-Part B* 42 (5) (2012) 1489–1500.
- [12] W.T. Freeman, E.C. Pasztor, O.T. Carmichael, Learning low-level vision, *Int. J. Comput. Vis.* 40 (1) (2007) 25–47.
- [13] W. Dai, O. Milenkovic, Subspace pursuit for compressive sensing signal reconstruction, *IEEE Trans. Inf. Theory* 55 (5) (2009) 2230–2249.
- [14] C.T. Tony, L. Wang, Orthogonal matching pursuit for sparse signal recovery with noise, *IEEE Trans. Inf. Theory* 57 (7) (2011) 4680–4688.
- [15] T. Do Thong, G. Lu, Nam Nguyen, D.T. Trac, Sparsity adaptive matching pursuit algorithm for practical compressed sensing, in: *Proceedings of the 42th Asilomar Conference on Signals, Systems, and Computers*, Pacific Grove, October 26–29, California, pp. 234–240, 2008.
- [16] Jarvis Haupt, Rob Nowak, Signal reconstruction from noisy random projections, *IEEE Trans. Inf. Theory* 52 (9) (2006) 4036–4048.
- [17] M. Protter, M. Elad, H. Takeda, Generalizing the nonlocal-means to super-resolution reconstruction, *IEEE Trans. Image Process.* 18 (1) (2009) 36–51.
- [18] R.Z. Zhao, X.X. Ren, X. Han, S.H. Hu, An improved sparsity adaptive matching pursuit algorithm for compressive sensing based on regularized backtracking, *J. Electron.* 29 (6) (2012) 580–584.
- [19] Y.C. Eldar, P. Kuppinger, H. Bolcskei, Compressed sensing of block-sparse signal: uncertainly relations and efficient recovery, *IEEE Trans. Signal Process.* 58 (6) (2010) 3042–3054.
- [20] Y.R. Li, D.Q. Dai, L. Shen, Multiframe super-resolution reconstruction using sparse directional regularization, *IEEE Trans. Circuits Syst. Video Technol.* 20 (7) (2010) 945–956.
- [21] E. Candès, J. Romberg, T. Tao, Robust uncertainty principles: exact signal reconstruction from highly incomplete frequency information, *IEEE Trans. Inf. Theory* 52 (2) (2006) 489–509.
- [22] W.T. Freeman, T.R. Jones, E.C. Pasztor, Example based super-resolution, *IEEE Comput. Graph. Appl.* 22 (2) (2002) 56–65.
- [23] K.I. Kim, Y.H. Kwon, Example-based learning for single-image super-resolution, in: *Proceedings of the 30th DAGM Symposium on Pattern Recognition*, Oct. 19–21, Munich, Germany, vol. 5096, pp. 456–465, 2008.
- [24] J. Pu, J.P. Zhang, P.H. Guo, Interactive super-resolution through neighbor embedding, *Lecture Notes in Computer Science, LNCS*, in: *Proceedings of the 9th Asian conference on Computer Vision, ACCV, Xi'an, China, 5996, 2010*, pp. 496–505.
- [25] M. Elad, D. Datsenko, Example-based regularization deployed to super-resolution reconstruction of a single image, *Comput. J.* 52 (1) (2008) 15–30.
- [26] C.V. Jiji, M. Joshi, S. Chaudhuri, Single-frame image super-resolution using learned wavelet coefficients, *Int. J. Imaging Syst. Technol.* 14 (3) (2004) 105–112.
- [27] C.V. Jiji, S. Chaudhuri, Single-frame image super-resolution through contourlet learning, *J. Appl. Signal Process.* 2006 (1) (2006) 1–11.
- [28] C. Wang, P. Xue, W. Lin, Improved super-resolution reconstruction from video, *IEEE Trans. Circuits Syst. Video Technol.* 16 (11) (2006) 1411–1422.
- [29] J.C. Yang, J. Wright, T. Huang, Y. Ma, Image super-resolution via sparse representation, *IEEE Trans. Image Process.* 19 (11) (2010) 2861–2873.
- [30] J.Z. Lu, Q.H. Zhang, Z.Y. Xu, Z.M. Peng, Image super-resolution reconstruction algorithm using over-complete sparse representation, *Syst. Eng. Electron.* 34 (2) (2012) 403–408.
- [31] Q. Xiao, X.H. Ding, S.J. Wang, Image denoising based on adaptive over-complete sparse representation, *Chin. J. Sci. Instrum.* 30 (9) (2009) 1886–1890.
- [32] D.L. Donoho, M. Elad, V.N. Temlyakov, Stable recovery of sparse overcomplete representation in the presence of noise, *IEEE Trans. Inf. Theory* 52 (1) (2006) 6–18.
- [33] M. Aharon, M. Elad, A. Bruckstein, K-SVD: an algorithm for designing over-complete dictionaries for sparse representation, *IEEE Trans. Image Process.* 54 (11) (2006) 4311–4322.
- [34] Y. Li, H.L. Gong, J.X. Liang, SAR image target feature extraction based on KSVD and PCA, *J. Jilin Univ. (Eng. Technol. Ed.)* 40 (5) (2010) 1336–1339.
- [35] L. Shang, P.G. Su, J. Chen, Millimeter wave image restoration based on fuzzy RBFNN and sparse representation, *J. Comput. Appl.* 32 (7) (2012) 1871–1874.
- [36] D. Needell, D. Vershynin, Uniform uncertainty principle and signal recovery via regularized orthogonal matching pursuit, *Found. Comput. Math.* 9 (3) (2009) 317–334.
- [37] R. Baxaniuk, Compressive sensing, *IEEE Signal Process. Mag.* 24 (4) (2007) 118–121.
- [38] C.H. Zheng, L. Zhang, Vincent To-Yee Ng, Simon Chi-Keung Shiu, D.S. Huang, Metasample-based sparse representation for tumor classification, *IEEE/ACM Trans. Comput. Biol. Bioinform.* 8 (5) (2011) 1273–1282.
- [39] E.J. Candès, J. Romberg, T. Tao, Stable signal recovery from incomplete and inaccurate measurements, *Commun. Pure Appl. Math.* 59 (2006) 1207–1223.
- [40] W.S. Dong, L. Zhang, G. Shi, Image deblurring and super-resolution by adaptive sparse domain selection and adaptive regularization, *IEEE Trans. Image Process.* 20 (7) (2011) 1838–1857.
- [41] L. Shang, P.G. Su, C.X. Zhou, Denoising millimeter wave image using contourlet and sparse coding shrinkage, *Laser Infrared* 41 (9) (2011) 1049–1053.
- [42] B. Li, D.S. Huang, Locally linear discriminant embedding: an efficient method for face recognition, *Pattern Recognit.* 41 (12) (2008) 3813–3821.
- [43] R. Baraniuk, V. Cevceher, M. Duarte, Model-based compressive sensing, *IEEE Trans. Inf. Theory* 56 (4) (2010) 1982–2001.
- [44] D. Capel, A. Zisserman, Computer vision applied to super-resolution, *IEEE Signal Process. Mag.* 20 (3) (2003) 75–86.
- [45] S. Farsiu, M. Robinson, M. Elad, P. Milanfar, Fast and robust multiframe super resolution, *IEEE T-IP* 13 (2004) 1327–1344.
- [46] D.L. Donoho, Compresses sensing, *IEEE Trans. Inf. Theory* 52 (4) (2006) 1289–1306.
- [47] H. Rauhut, On the impossibility of uniform sparse reconstruction using greedy methods, *Sampl. Theory Signal Image Process.* 7 (2) (2008) 197–215.
- [48] D.S. Huang, H.J. Yu, Normalized feature vectors: a novel alignment-free s' uence comparison method based on the numbers of adjacent amino acids, *IEEE/ACM Trans. Comput. Biol. Bioinform.* 10 (2) (2013) 457–467.
- [49] S.L. Wang, Y.H. Zhu, W. Jia, D.S. Huang, Robust classification method of tumor subtype by using correlation filters, *IEEE/ACM Trans. Comput. Biol. Bioinform.* 9 (2) (2012) 580–591.
- [50] X.F. Wang, D.S. Huang, H. Xu, An efficient local Chan-Vese model for image segmentation, *Pattern Recognit.* 43 (3) (2010) 603–618.
- [51] S.S. Huang, J.B. Zhu, Recovery of sparse signals using OMP and its variants: convergence analysis based on RIP, *Inverse Probl.* 27 (3) (2011) 35003–35016.
- [52] J. Tropp, A. Gilbert, Signal recovery from random measurements via orthogonal matching pursuit, *IEEE Trans. Inf. Theory* 53 (12) (2008) 4655–4666.
- [53] M.J. Sun, N.Z. Feng, Y. Shen, Photoacoustic image reconstruction based on Bayesian compressive sensing algorithm, *Chin. Opt. Lett.* 9 (9) (2011) 44–47.
- [54] Y.R. Li, D.Q. Dai, Color super-resolution reconstruction and demosaicing using elastic net and tight frame, *IEEE Trans. Circuits Syst.* 50 (11) (2008) 3500–3512.
- [55] Y. Lu, L. Shen, Y. Xu, Multi-parameter regularization methods for high-resolution image reconstruction with displacement errors, *IEEE Trans. Circuits Syst. I* 54 (8) (2007) 1788–1799.



Li Shang received the B.Sc. degree and M.Sc. degree in Xi'an Mine University in June 1996 and June 1999, respectively. And in June 2006, she received the Doctor's degree in Pattern Recognition & Intelligent System in University of Science & Technology of China (USTC), Hefei, China. From July 1999 to July 2006, she worked at USTC, and applied herself to teaching. Now, she works at the Department of Communication Technology, Electronic Information Engineering College, Suzhou Vocational University. At present, her research interests include Image processing, Artificial Neural Networks and Intelligent Computing.



Yan Zhou received the B.Sc. degree and M.Sc. degree in China University of Geosciences in June 2003 and June 2006, respectively. She is currently pursuing the Ph.D. degree at the School of Electronics and Information Engineering of Soochow University, in the area of signal and information processing. From July 2006 to now, she works at the Department of Communication Technology, Electronic Information Engineering College, Suzhou Vocational University. At present, her research interests include Speech Signal Processing, Artificial Neural Networks and Intelligent Computing.



Xin Wang received the B.Sc. degree in Zhejiang University, China in July 2011. From July 2011 to July 2013, he worked as a research assistant at the College of Computer Science and Technology, Zhejiang University. He is currently pursuing the Ph.D. degree at the School of computing science of Simon Fraser University in Canada, in the area of Social Network and Recommender Systems. At present, his research interests include Machine Learning, Pattern Recognition, Recommender Systems and Social Networks.



Zhanli Sun received the Ph.D. degree from the University of Science and Technology of China, in 2005. Since 2006, he has worked with The Hong Kong Polytechnic University, Nanyang Technological University, and National University of Singapore. Now, he is currently a Professor with School of Electrical Engineering and Automation, Anhui University, China. His research interests include Machine Learning, Pattern Recognition, and Image and Signal Processing.